24th Australasian Fluid Mechanics Conference - AFMC2024
Canberra, Australia
1-5 December 2024
Paper No: AFMC2024-180

Comparison of turbulent boundary layer streamwise development over two- and three-dimensional rough surfaces

Jiahao Kong[1*], Bagus Nugroho[2], Luke Bennetts[3] and Rey Chin[1]

[1] School of Electrical and Mechanical Engineering, University of Adelaide, South Australia 5005, Australia
[2] Department of Mechanical Engineering, University of Melbourne, Melbourne, 3010 Victoria, Australia
[3] School of Computer and Mathematical Sciences, University of Adelaide, Adelaide, 5005 South Australia, Australia
*mailto: Jiahao.kong@adelaide.edu.au

Abstract

Turbulent boundary layers (TBLs) above two-dimensional (2D) square-bar and three-dimensional (3D) sandpaper roughness are studied experimentally to investigate streamwise development and Reynolds number effects for two types of roughness. Previous studies have studied 2D square-bar roughness and 3D sandpaper roughness separately. There is a need to perform rough wall TBL measurements and systematical comparisons for 2D and 3D roughness. In this study, we performed TBL measurements over 2D and 3D rough walls at various streamwise stations spanning from $x = 0.62$ m to 1.90 m, and we operated at various free-stream velocities to obtain Reynolds numbers ranging from $Re_\tau \approx 1500$ to 5500. The roughness heights from peak to valley of 2D and 3D roughness are similar, with $k = 1.5$ mm and 1.219 mm, respectively. The mean velocity and turbulence intensity profiles of the two rough-wall TBLs show a consistent streamwise development with the literature results. The turbulent intensity profiles show the outer region collapsing at a wall-normal position farther away from the wall for the 2D roughness, compared with the 3D roughness result. In addition, the 2D roughness TBL shows a higher skewness than the 3D result in the near-wall region. The streamwise development of the turbulence intensity and turbulence energy distribution for 2D and 3D roughness are revealed in the analysis.

1 Introduction

Turbulent boundary layer flows (TBLs) are important in many practical applications and are widely observed over airfoils and ship hulls. The characteristics of TBLs have been investigated extensively above a smooth wall over the last decade (Marusic *et al.*, 2010). However, most of the bounding walls in practical applications are considered as rough walls when the topographical parameters are large enough to disrupt the laminar sublayer, imposing dynamically significant perturbation in near-wall flows. For example, when the roughness element is tall enough to protrude into the buffer layer, form drag is distributed on the individual elements and added to the skin friction drag, which causes higher wall drag than the smooth wall.

Rough walls can be classified into two-dimensional (2D) roughness for their simplicity and three-dimensional (3D) roughness, which is close to the realistic roughness. The typical 2D roughness is associated with transverse-aligned elements (square bars) with regular streamwise distribution, while 3D roughness is typified by sand-grain type roughness. TBL flows above sandpaper have been performed experimentally at different streamwise locations and free-stream velocities to investigate the streamwise development and the Reynolds number influence (Squire *et al.*, 2016). In the mean statistics of streamwise velocity defect, variance and skewness, the roughness effects are confined within the inner 20% of the boundary layer thickness. The outer layer shows a collapse for the mean statistics at high friction Reynolds numbers $Re_\tau > 14000$ with the smooth-wall TBLs, which supports the critical concept of Townsend's outer layer similarity.

The square-bar 2D roughness has been used as a simplified model to study the roughness effect by experiments and numerical simulations (Lee & Sung, 2007; Efros & Krogstad, 2011; Djenidi *et al.*, 2018). The results of those 2D roughness studies have shown that 2D roughness not only affects the roughness sublayer but also extends to the outer layer in comparison to the smooth-wall TBL, particularly the increase in normalised turbulence intensity (Krogstad & Antonia, 1999; Lee & Sung, 2007; Volino *et al.*, 2009). The roughness effect in the outer layer has been observed in a wide range of Reynolds numbers from $Re_\tau = 500$ (Lee & Sung, 2007) to 13000 (Efros & Krogstad, 2011), contrary to the outer layer similarity. The numerical results of Lee & Sung (2007) suggested that the large-scale motions produced by 2D roughness are much larger than those of 3D

roughness due to the spanwise blockage effect of 2D roughness. In addition, Djenidi *et al.* (2018) suggested that the interaction between the 2D roughness and the outer layer is related to the roughness geometry ratio, e.g. the ratio δ_{99}/k_s, where δ_{99} is the boundary layer thickness (based on 99% of the free-stream velocity) and k_s is the equivalent sandgrain roughness. The effects of Reynolds number and roughness geometry ratio δ_{99}/k_s for the regular 2D and irregular 3D roughness have been studied by Djenidi *et al.* (2018) and Squire *et al.* (2016), respectively. However, there is a lack of studies systematically examining the roughness effects in the outer layer for 2D and 3D rough-wall TBLs, including the statistics of turbulence energy spectra and skewness. The 2D and 3D roughness effects in TBL streamwise development need to be investigated and analysed systematically by performing 2D and 3D rough-wall TBL measurements at various Reynolds numbers.

The present study aims to investigate the 2D and 3D roughness effects by performing TBL experiments over typical 2D and 3D rough walls at various streamwise stations and free-streamwise velocities, leading to a change in the ratio of boundary layer thickness to equivalent sandgrain roughness height δ_{99}/k_s and Reynolds numbers, respectively. The present study investigated the mean statistics, including the mean velocity, skewness and turbulent intensity profiles. Finally, the premultiplied energy spectra of the streamwise velocity for the streamwise development of rough-wall TBLs are analysed.

2 Experimental Condition

Experiments were performed in a closed-loop wind tunnel at the University Adelaide. The test section was 2 m long and had a rectangular cross-sectional area of $0.5 \times 0.3\,\mathrm{m}^2$. The sidewalls were adjusted to maintain zero pressure gradient (ZPG) along the test section with a range of free-stream velocities up to $U_\infty = 24\,\mathrm{m\,s^{-1}}$. The boundary layer was tripped at the leading edge using a 36-grit sandpaper of 100 mm in length to accelerate the TBL flow development.

For rough wall configuration, a typical 2D roughness was made by transversely affixing ABS plastic square bars on the aluminium plate downstream of the tripping device. The bar height was $k = 1.5\,\mathrm{mm}$, and the streamwise spacing was $p = 8k$, similar to the numerical and experimental studies (Lee & Sung, 2007; Kong *et al.*, 2023). This streamwise spacing was chosen because it is a typical 2D roughness configuration to produce the maximum wall drag. The surface elevation h for the 2D roughness is obtained from the numerical modelling and used to determine the roughness parameters across the whole roughness area of 500mm $\times$ 2000mm. For 3D roughness, 36-grit sandpaper was used, the same as the tripping device, which extends to the same distance as the square-bar roughness. The roughness surface elevation h is measured from an optical profilometer over a 25.4mm $\times$ 25.4mm area (see Squire *et al.* (2016)). The roughness parameters for two rough walls are summarised in Table 1.

Roughness parameter	2D	3D	**Units**	**Formula**
k	1.5	1.219	mm	max h' - min h'
k_a	0.188	0.119	mm	$\overline{\lvert h' \rvert}$
k_{rms}	0.509	0.150	mm	$\sqrt{\overline{h'^2}}$
k_{ku}	5.684	3.128	–	$\overline{h'^3}/\overline{h^3_{rms}}$
k_{sk}	2.268	0.093	–	$\overline{h'^4}/\overline{h^4_{rms}}$
ES_x	0.249	0.482	–	$\lvert\overline{\frac{dh'}{dx}}\rvert$

Table 1. Geometrical parameters for square-bar and sandpaper roughness. h' is the roughness height deviation, $h' = h - \overline{h}$.

The measurements were taken at a range of streamwise stations from $x = 0.62\,\mathrm{m}$ to 1.9 m and operated at two free-stream velocities for two sets of rough-wall TBLs. For the 2D roughness measurement, the five streamwise locations are in the middle of two adjacent roughness bars, and two free-stream velocities $U_\infty = 11$ and $20\,\mathrm{m\,s^{-1}}$ are performed. The 3D rough-wall TBLs are also measured at five streamwise locations and operated at $U_\infty = 14$ and $20\,\mathrm{m\,s^{-1}}$. Four cases of rough-wall TBLs are measured for two roughness at low and high Reynolds numbers. The experimental conditions for the rough-wall measurements are summarised in Table 2. A smooth-wall TBL measurement was also performed using the same flow facility as the rough-wall measurements at $x = 1.9\,\mathrm{m}$ and operated at $U_\infty = 20\,\mathrm{m\,s^{-1}}$. The bottom floor is covered with a flat aluminium

plate. Additional two smooth-wall TBL results of Marusic *et al.* (2015) at higher friction Reynolds number $Re_\tau = 2182$ and 4682 are used for comparison. Note that the letters of the case name, "2D", "3D", and "S" denotes the 2D, 3D and smooth walls, and the last letters, "L", "M", and "H", denote low, medium and high Reynolds numbers, respectively.

Case	x (mm)	U_∞ (m s^{-1})	Re_τ	δ_{99} (mm)	U_τ (m s^{-1})	ΔU^+	k_s^+	δ_{99}/k_s	$c_f \times 10^3$	l^+	Sym
	620	11	1570	31.9	0.7473	11.1	381.0	4.12	9.0	24.6	□
	690	11	1700	34.7	0.7477	11.2	381.2	4.46	8.9	24.7	□
2DL	850	11	1850	38.6	0.7272	11.1	370.8	4.99	8.5	24.0	□
	1150	11	2200	47.6	0.7010	11.0	357.4	6.16	8.0	23.1	□
	1900	11	2960	68.2	0.6593	10.8	336.3	8.80	7.2	21.7	□
	1075	14	1500	31.0	0.7376	7.0	62.3	24.08	5.6	24.3	▽
	1150	14	1520	31.9	0.7249	6.8	61.2	24.83	5.4	23.9	▽
3DL	1300	14	1580	34.2	0.7007	6.4	59.2	26.71	5.2	23.1	▽
	1600	14	1870	40.7	0.6976	6.5	58.9	31.8	5.0	23.0	▽
	1900	14	2080	45.5	0.6927	6.6	58.49	35.6	4.9	22.8	▽
	620	20	2830	31.0	1.3849	12.8	742.4	3.82	9.7	45.7	◇
	690	20	3040	33.6	1.3724	12.7	714.6	4.26	9.4	45.3	◇
2DH	850	20	3350	38.1	1.3333	12.5	665.9	5.03	8.8	44.0	◇
	1150	20	3960	47.1	1.2750	12.3	604.8	6.55	8.1	42.1	◇
	1900	20	5500	69.6	1.1918	12.1	553.1	9.89	7.2	39.3	◇
	1075	20	2200	32.0	1.0495	7.7	77.5	28.61	5.5	34.6	△
	1150	20	2220	32.8	1.0270	7.5	75.9	29.26	5.3	33.9	△
3DH	1300	20	2350	35.3	1.0092	7.3	74.6	31.56	5.2	33.3	△
	1600	20	2660	41.1	0.9802	7.0	72.4	36.72	4.8	32.3	△
	1900	20	3110	48.5	0.9724	7.1	71.7	43.39	4.7	32.1	△
SL	1900	20	1836	37.0	0.7521	-	-	-	2.8	24.8	– –
SM	2650	20	2182	45.0	0.7342	-	-	-	2.7	26.1	– –
SH	6300	20	4682	103.0	0.6880	-	-	-	2.3	24.5	– –

Table 2. Boundary layer condition detail of the four rough-wall experiments and three smooth-wall results. The cases of SM and SH refer to Marusic *et al.* (2015).

Hot-wire anemometry (HWA) was used to measure TBL from the near-wall position to the free-stream flow at $y = 1.5\delta_{99}$. Note that the origin of y is defined at the crest of roughness elements. The HWA sensors were single-wire boundary-type probes with a Wollaston filament of $d = 2.5\,\mu$m diameter and $l = 0.51$ mm length to maintain the length-to-diameter ratio $l/d \geq 200$. The inner-scaled sensor length $l^+ = l \times U_\tau/\nu$ ranges from 21.7–26.1 for the low Reynolds number rough-wall cases (2DL and 3DL) and the three smooth-wall cases, which indicates that those cases do not experience significant spatial attenuation (Hutchins *et al.*, 2009). The l^+ values for the high Reynolds number cases (2DH and 3DH) are maintained from 32.1–45.7, which is below the suggested $l^+ = 50$–60 to perform well-resolved outer-layer turbulence intensity profiles (Hutchins *et al.*, 2009). The velocity signal from HWA was sampled with frequency $f_s = 51200$ Hz and duration $T = 120$ s using a National Instrument data acquisition board (USB-NI6211). Note that the largest scales of turbulent structures are observed to exceed 20δ (Adrian *et al.*, 2000), hence, the sampling duration is required to encompass several hundreds of these large-scale events for the converged statistics ($TU_\infty/\delta_{99} > 20000$). The calibration was performed before and after each TBL profile measurement by locating a Pitot tube above the hot-wire probes, approximately 10 mm into the free-stream flow. The pitot tube was used with an electronic barometer (220DD Baratron, MKS) to determine the calibration velocity. The temperature condition was also monitored by an RTD-type thermocouple (PT1000) to compensate for the temperature drift of the HWA signal. Fourth-order polynomial curves were used to fit the pressure data and hot-wire voltage signals. Linear interpolation was made to correct the temperature drift between pre- and post-calibration profiles.

Friction velocity U_τ is critical for the rough-wall TBL analysis because it is required in the inner-scale normalisation $U^+ = U/U_\tau$ and $y^+ = y \times U_\tau/\nu$. For all rough-wall TBL results, this study employed the modified clauser method (Perry & Li, 1990), which has been used for TBLs over square-bar and sandpaper roughness by Kong *et al.* (2023) and Squire *et al.* (2016), respectively. The technique plots the profiles of U/U_∞ versus

$(y')/\delta^*$, where δ^* is the displacement boundary layer thickness and $y' = y + \varepsilon$ (ε is the roughness offset). The measurement data in the logarithmic region should follow the following equation,

$$\frac{U}{U_\infty} = \frac{1}{\kappa}\frac{U_\tau}{U_\infty}\ln\left(\frac{y'}{\delta^*}\right) + C, \tag{1}$$

where $C = f(\frac{U_\tau}{U_\infty}, \Pi)$ is the intercept constant of the line. Several iterations were made by applying the first-order polynomial fit to evaluate a constant line. The slope of the constant line providing the least square error fitting can be used to determine U_τ. The log region is well defined within the range from $y'^+ = 3\sqrt{Re_\tau}$ to $y'/\delta_{99} = 0.19$ for smooth-wall TBLs Marusic *et al.* (2013). However, the log region bounds for rough-wall TBLs are still arguable and under investigation. In this study, the bounds of the log region are suggested from $y'^+ = 3.4\sqrt{Re_\tau}$ to $y'/\delta_{99} = 0.19$ for square-bar and sandpaper roughness by Kong *et al.* (2023) and Squire *et al.* (2016). For simplicity, the roughness offset is fixed at half the roughness element height, $\varepsilon = k/2$, and the von Karman constant $\kappa = 0.41$ here (Djenidi *et al.*, 2018; Squire *et al.*, 2016). The accuracy of U_τ estimated via the modified Clauser method (for rough wall TBLs) has been investigated by Flack *et al.* (2007), and its uncertainty is around 3 – 5%.

3 Result and Discussion

Figure 1 shows the development of mean velocity profiles for 2D and 3D roughness by streamwise propagation and increasing free-streamwise velocity. The smooth-wall TBL profiles at $Re_\tau = 3000$ and 6000 are included as reference profiles from Marusic *et al.* (2015). In Figures 1(a,b), the profiles of 2D roughness are located lower than those of 3D roughness, which is consistent with the value ranges of the roughness function, the downward shifting of the log region from the smooth-wall profile, $\Delta U^+ \approx 11$ and 7 for 2D and 3D roughness, respectively. The roughness function ΔU^+ is approximately constant for each set of rough-wall TBLs with streamwise development. The outer edge of mean velocity profiles U_∞^+ increases with streamwise development, which reflects that the friction coefficient $c_f = 2/U_\infty^{+2}$ decreases over 2D and 3D rough walls along with streamwise development. At the two streamwise locations, Figures 1 (c,d) show that the the roughness function ΔU^+ increases and U_∞^+ remains approximately constant with increasing free-streamwise velocity, which causes the profile to shift to the left. The rough-wall TBL is usually considered fully rough with this trend (Djenidi *et al.*, 2018). The result indicates that the roughness function is dependent on the geometrical parameters (k_s) and increases with increasing Reynolds numbers by increasing U_∞, and shows independence on the streamwise location (also the ratio of δ_{99}/k_s). In contrast, the friction coefficient decreases with increasing δ_{99}/k_s, but is not affected by the increase in Reynolds numbers caused by increasing U_∞, which is consistent with the results of the sandpaper roughness study by (Squire *et al.*, 2016). The comparison of 2D and 3D roughness indicates that both rough walls show similar behaviour with increases in δ_{99}/k_s and Re_τ, and the values of ΔU^+ and c_f for the 2D roughness are commonly larger than the 3D roughness.

The streamwise velocity skewness profiles for the four sets of rough-wall results are separately plotted for two streamwise locations in Figure 2. The skewness factor of streamwise velocity fluctuation ($\mathrm{Sk} = \overline{u'^3}/\overline{u'^2}^{3/2}$) quantifies the asymmetry of the distribution of streamwise velocity fluctuations. In Figure 2 (a), the rough-wall skewness profiles collapse with the smooth-wall profiles beyond $y'/\delta_{99} \approx 0.2$, and such collapsing point becomes closer to the wall at $y'/\delta_{99} \approx 0.06$ along with streamwise development (increasing δ_{99}/k_s). In the near-wall region, the skewness factor of the rough-wall results is positive and larger than the zero skewness of the smooth wall, indicating that rough walls lead to more positive velocity fluctuations. The comparison of two rough wall results implies that the 2D roughness can cause more positive velocity fluctuation than the 3D roughness in the near-wall region. It is worth noting that the near-wall shape of the skewness profile correlates with the type of roughness related to k_s. The left shifting of the near-wall skewness profile for each type of roughness is associated with the increase in δ_{99}/k_s. Therefore, the skewness profile is dominated by k_s and influenced by δ_{99}/k_s in the near-wall region.

The inner-scaled turbulence intensity profiles are plotted on an outer-scaled abscissa in Figure 3 to investigate the outer-layer similarity in the turbulence intensity. As baseline flows, the smooth wall profiles have a near-wall peak resulting from the highly energetic near-wall cycle of streaks and quasi-streamwise vortices (Hutchins *et al.*, 2007). For the rough wall results, the magnitude of the inner peak diminishes, which is generally associated with the disturbance of the near-wall cycle of streaks and quasi-streamwise vortices (Schultz & Flack, 2007). The streamwise development of the turbulence intensity is similar for two roughness types

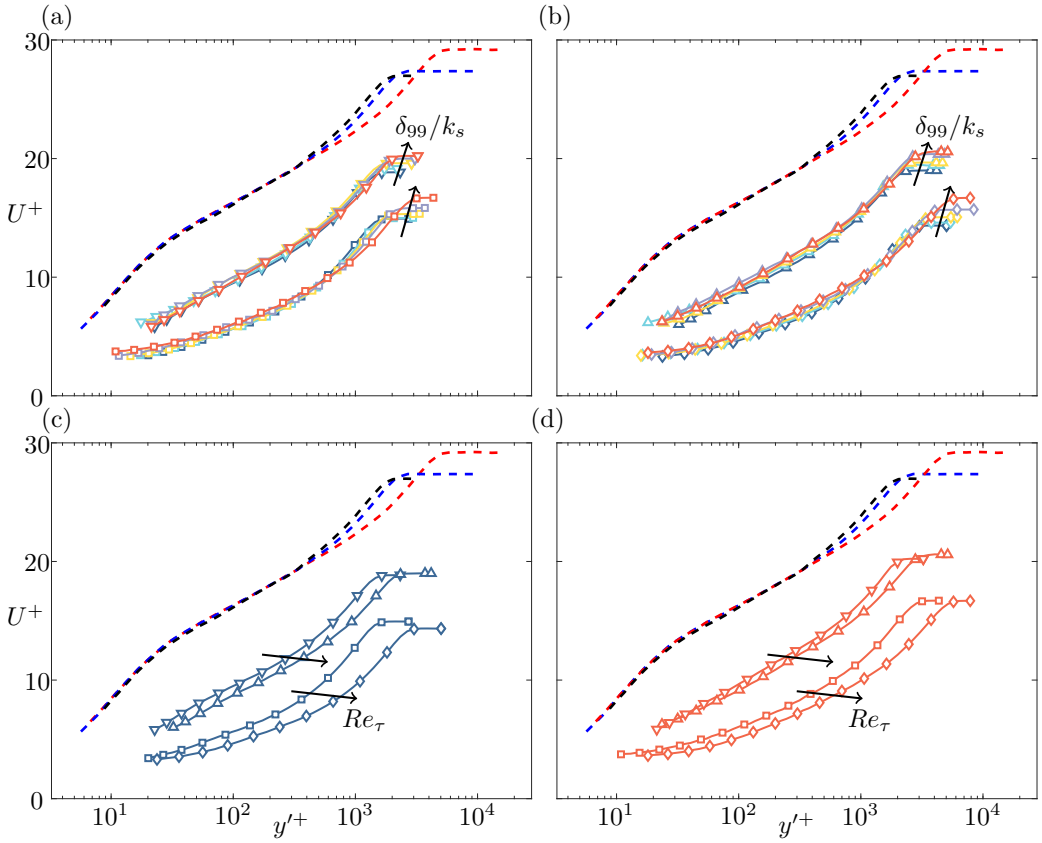

Figure 1. Comparison of mean velocity profiles for the cases of 2DL and 3DL (a) and 2DH and 3DH (b), and the four cases at upstream (c) and downstream (d) stations. Dashed black, blue and red profiles are smooth-wall TBL results at $Re_\tau = 1800$, 2200 and 4700, respectively. The arrows denote an increase of δ_{99}/k_s (a,b) and Re_τ (c,d), respectively. The symbol for the four sets of rough-wall results and color code for five streamwise stations refer to Table 2.

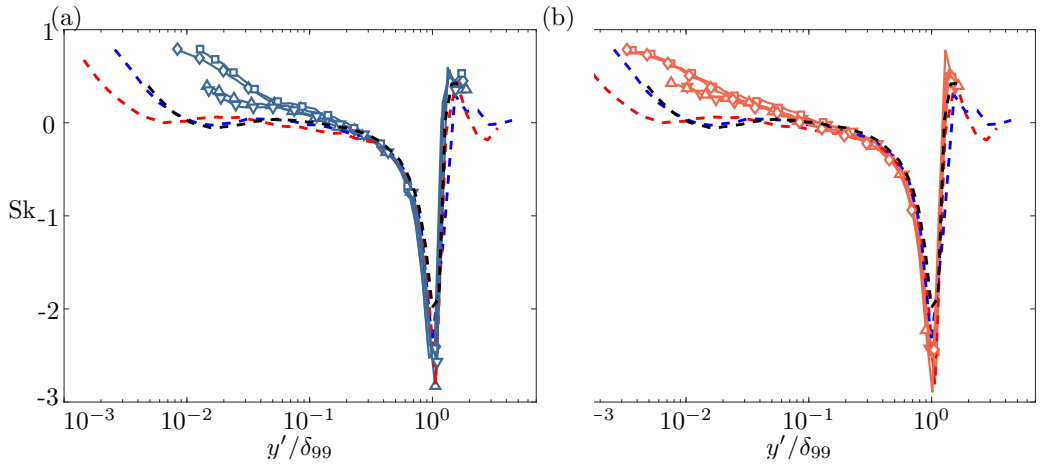

Figure 2. Streamwise skewness profiles for the four set of rough-wall TBLs at upstream (a) and downstream (b) locations. Dashed black, blue and red profiles are smooth-wall TBL results at $Re_\tau = 1800$, 2200 and 4700, respectively.

and different Reynolds numbers, demonstrating a trend that the inner-layer turbulence intensity increases along with streamwise development and the outer-layer turbulence intensity collapse. In Figure 3 (b), the comparison of 2DH and 3DH shows that the 2D roughness profiles are higher than those of 3D roughness. Considering the overall U_τ of 2DH is higher than that of 3DH, the turbulence intensity of 2D rough-wall TBLs without inner scaling is still higher than that of 3D roughness at the same free-stream velocity.

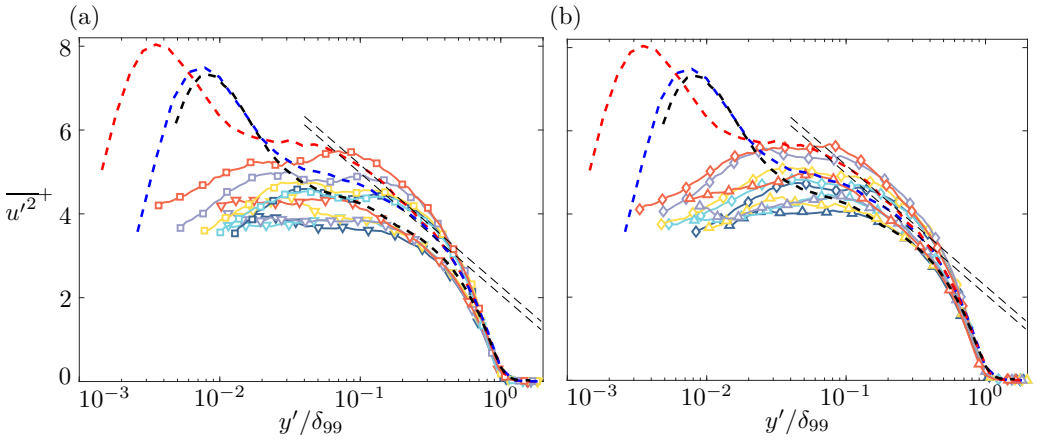

Figure 3. The inner-scaled turbulence intensity profiles for 2DL and 3DL (a) and 2DH and 3DH (b). Dashed black, blue and red profiles are smooth-wall TBL results at $Re_\tau = 1800$, 2200 and 4700, respectively. The dashed lines denote the bounds of the logarithmic profile Eq 2 with $B_1 = 2.07$–2.27.

The outer-layer similarity hypothesis describes a logarithmic profile in the turbulence intensity as below,

$$\overline{u'^2}^+ = B_1 - A_1 \log(y'/\delta_{99}). \tag{2}$$

The constant $A_1 = 1.26$ is considered to be universal (Marusic *et al.*, 2013), and B_1 is suggested to become approximately convergent with 2.17 for smooth-wall TBLs at $Re_\tau \geq 4000$ (Squire *et al.*, 2016). Figure 3 shows the logarithmic layer of two smooth-wall cases, SM and SH, collapsing and following the dashed band at $Re_\tau \geq 2200$. Compared to the smooth-wall TBLs, the 2D rough-wall profiles are higher, and the 3D results are lower for low and high Reynolds numbers in Figures 3(a) and (b), respectively. For rough-wall TBLs, the logarithmic region in the turbulence intensity is not clear enough at the studied range of Reynolds numbers due to the roughness effect. Such logarithmic profile for the turbulence intensity can be estimated by fitting the logarithmic profile at the onset bound of the log region defined in the mean velocity profile, $y'^+ = 3.4\sqrt{Re_\tau}$ (Squire *et al.*, 2016). The constant B_1 estimated at this onset location of the logarithmic region can be used to quantify the roughness effects on turbulence intensity in the outer region. The value of B_1 is plotted with Re_τ, k_s^+ and δ_{99}/k_s in Figure 4. For 3D roughness, the constant B_1 increases with increasing Re_τ and k_s^+ but does not correlate with δ_{99}/k_s, which is consistent with the finding of Squire *et al.* (2016). In contrast, the constant B_1 of 2D roughness seems to be a function of Re_τ and δ_{99}/k_s and asymptotically converges to a value at $B_1 \approx 2.7$. This output confirms that the 2D roughness effect of increasing turbulence intensity can extend to the outer layer farther away from the wall than that of 3D roughness.

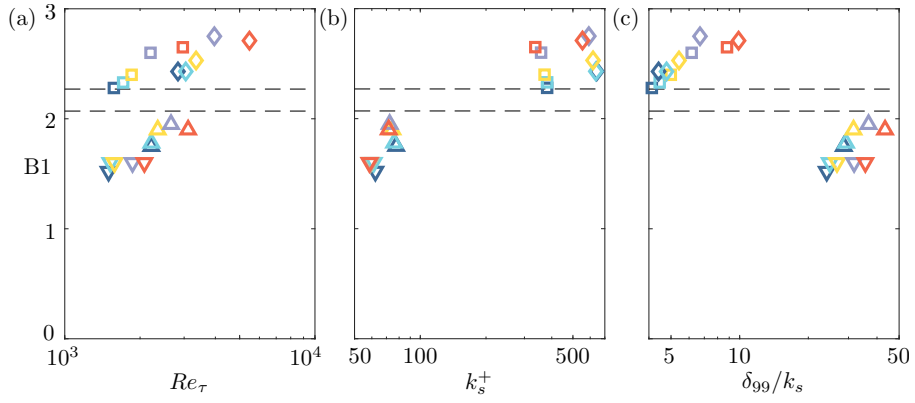

Figure 4. Correlations of B_1 with Re_τ, k_s^+ and δ_{99}/k_s. The dashed bounds show $B_1 = 2.17 \pm 0.1$.

Pre-multiplied energy spectra maps of the streamwise velocity fluctuation, $k_x\phi_{uu}^+$, are plotted along streamwise development for the high–Re_τ cases of 2DH and 3DH in Figure 5. The spatial energy spectra ϕ_{uu} are computed by deducing the spatial flow field of streamwise velocity fluctuations from the temporally sampled measurements using Taylor's hypothesis (Taylor, 1938). The spectra are premultiplied by the streamwise

wavenumber, $k_x = 2\pi f/U_c$, where f is the frequency and the convection velocity U_c, is assumed to be equal to the local mean streamwise velocity (Monty *et al.*, 2011). The spectra are scaled by the friction velocity U_τ and plotted against the normalised streamwise wavelength, $\lambda_x^+ = (2\pi/k_x)/(\nu/U_\tau)$. For 2D roughness, most turbulence energy is from the outer-peak larger-scale structures with $\lambda_x^+ \approx 1 \times 10^4$. Figures 5(a–d) show that overall structures from the wall to the outer layer grow with more normalised turbulence energy with streamwise development. The 3D roughness has a similar trend of streamwise development to the 2D roughness, which clearly shows that more turbulence energy resides in the inner and outer peaks.

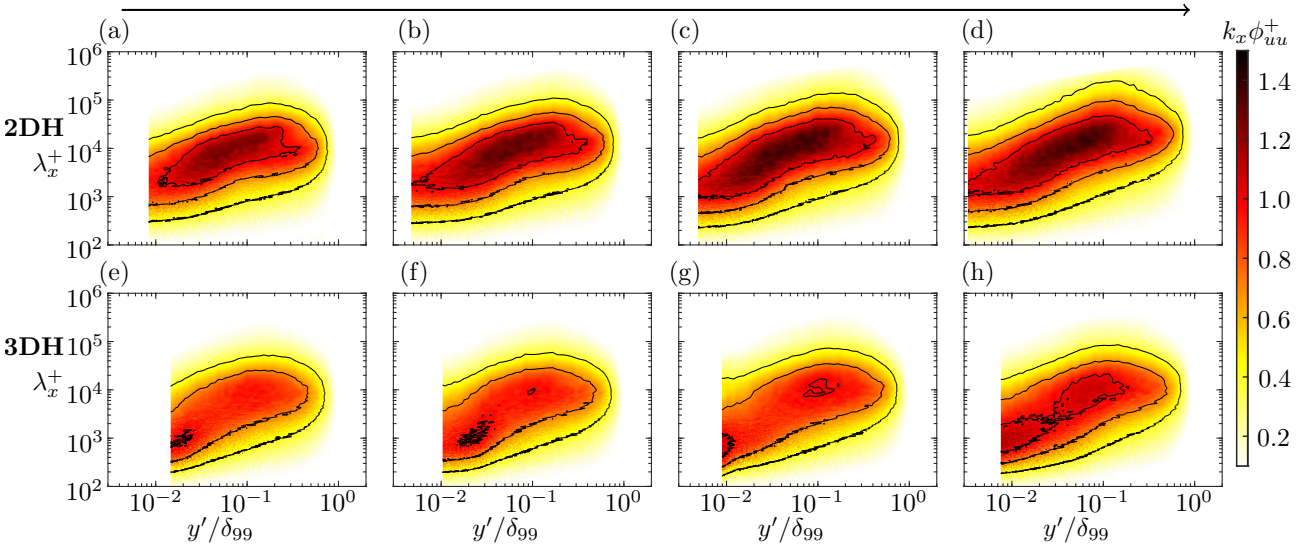

Figure 5. Pre-multiplied spectra contour for streamwise development of 2DH (a–d) and 3DH (e–h). The black contour lines denote to $k_x\Phi_{uu}^+ = 0.4, 0.7$ and 1. The top arrow indicates the streamwise development direction.

4 Conclusions

The experimental study of rough-wall TBLs over two types of roughness, including the 2D regular square-bar and 3D sandpaper roughness. TBL measurements are performed at streamwise stations and different free-stream velocities to investigate the streamwise development and Reynolds number effect for two types of roughness. The roughness function depends on the roughness topography related to k_s, and also increases with Re_τ by increasing U_∞. The skewness factor is also influenced by roughness in the near-wall region. The near-wall skewness increases with an increase in k_s, but shows independence on increasing Re_τ. For the streamwise development of turbulence intensity, the inner-layer turbulence intensity increases along with streamwise distance, consistent with the spectra energy results. This streamwise development trend is similar for two types of roughness and different Reynolds numbers. Moreover, 2D roughness can induce stronger turbulence intensity and extend to the outer layer farther away from the wall than that of 3D roughness. For the range of Reynolds numbers studied in this study, the turbulence intensity is higher and lower than the smooth-wall result at $y'/\delta_{99} \approx 0.4$ for 2D and 3D roughness, respectively. The variation in turbulence intensity for 2D roughness appears to correlate with Re_τ and δ_{99}/k_s, while that of 3D roughness seems related with Re_τ and k_s^+.

Acknowledgments

The authors wish to thank Australian Research Council (ARC) for the financial support for this research.

References

Marusic, I., McKeon, B. J., Monkewitz, P. A., Nagib, H. M., Smits, A. J. and Sreenivasan, K. R. 2010, Wall-bounded turbulent flows at high Reynolds numbers: Recent advances and key issues, *Physics of Fluids*, **22(6)**, 1–24.

Squire, D. T., Morrill-Winter, C., Hutchins, N., Schultz, M. P., Klewicki, J. C. and Marusic, I. 2016, Comparison of turbulent boundary layers over smooth and rough surfaces up to high Reynolds numbers, *Journal of Fluid Mechanics*, **795**, 210–240.

Lee, S. H. and Sung, H. J. 2007, Direct numerical simulation of the turbulent boundary layer over a rod-roughened wall. *Journal of Fluid Mechanics*, **584**, 125–146.

Efros, V. and Krogstad, P. Å. 2011, Development of a turbulent boundary layer after a step from smooth to rough surface. *Experiments in Fluids*, **51(6)**, 1563–1575.

Volino, R. J., Schultz, M. P. and Flack, K. A. (2009). Turbulence structure in a boundary layer with two-dimensional roughness. *Journal of Fluid Mechanics*, **635**, 75–101.

Djenidi, L., Talluru, K. M. and Antonia, R. A. 2018, Can a turbulent boundary layer become independent of the Reynolds number? *Journal of Fluid Mechanics*, **851**, 1–22.

Kong, J., Bennetts, L. G., Nugroho, B. and Chin, R. C. 2023, Systematic study of the Reynolds number and streamwise spacing effects in two-dimensional square-bar rough-wall turbulent boundary layers. *Physical Review Fluids*, **8(1)**, 014601.

Krogstad, P. Å. and Antonia, R. A. 1999, Surface roughness effects in turbulent boundary layers. *Experiments in Fluids*, **27(5)**, 450–460.

Adrian, R. J., Meinhart, C. D. and Tomkins, C. D. 2000, Vortex organization in the outer region of the turbulent boundary layer. *Journal of Fluid Mechanics*, **422**, 1–54.

Hutchins, N., Nickels, T. B., Marusic, I. and Chong, M. S. 2009, Hot-wire spatial resolution issues in wall-bounded turbulence. *Journal of Fluid Mechanics*, **635**, 103–136.

Perry, A. E. and Li, J. D. 1990, Experimental support for the attached-eddy hypothesis in zero-pressure-gradient turbulent boundary layers. *Journal of Fluid Mechanics*, **218**, 405–438.

Flack, K. A., Schultz, M. P. and Connelly, J. S. 2007, Examination of a critical roughness height for outer layer similarity. *Physics of Fluids*, **19(9)**, 95104.

Marusic, I., Chauhan, K. A., Kulandaivelu, V. and Hutchins, N. 2015, Evolution of zero-pressure-gradient boundary layers from different tripping conditions. *Journal of Fluid Mechanics*, **783**, 379–411.

Volino, R. J., Schultz, M. P. and Flack, K. A. 2009, Turbulence structure in a boundary layer with two-dimensional roughness. *Journal of Fluid Mechanics*, **635**, 75–101.

Schultz, M. P. and Flack, K. A. 2007, The rough-wall turbulent boundary layer from the hydraulically smooth to the fully rough regime. *Journal of Fluid Mechanics*, **580**, 381–405.

Marusic, I., Monty, J. P., Hultmark, M. and Smits, A. J. 2013, On the logarithmic region in wall turbulence. Journal of Fluid Mechanics, **716**, R3.

Taylor, G. I. 1938, The Spectrum of Turbulence. *Proceedings of the Royal Society of London. Series A - Mathematical and Physical Sciences*, **164(919)**, 476–490.

Monty, J. P., Allen, J. J., Lien, K. and Chong, M. S. 2011, Modification of the large-scale features of high Reynolds number wall turbulence by passive surface obtrusions. *Experiments in Fluids*, **51(6)**, 1755–1763.